Fine Structure of Proton-Neutron Mixed Symmetry States in Some $N = 80$ Isotones

Ch. Stoyanov[1], N. Lo Iudice[2], and D. Tarpanov[1]

[1] Institute for Nuclear Research and Nuclear Energy, 1784 Sofia, Bulgaria,
[2] Dipartimento di Scienze Fisiche, Universitá di Napoli "Federico II"
and Istituto Nazionale di Fisica Nucleare,
Monte S Angelo, Via Cintia I-80126 Napoli, Italy

Abstract. A microscopic multiphonon approach is adopted to investigate the structure of some low-lying states observed experimentally in the $N = 80$ isotones ^{134}Xe, ^{136}Ba and ^{138}Ce. The calculation yields levels and electromagnetic transition strengths in good agreement with experiments and relates the observed selection rules to the neutron-proton symmetry and phonon content of the observed states. Moreover, it ascribes the splitting of the $M1$ strength in ^{138}Ce to the proton subshell closure which magnifies the role of pairing in the excitation mechanism.

1 Introduction

Low-energy spectra in nuclei are of crucial importance for understanding the correlations among valence nucleons. They include elementary excitations, like the low-lying 2^+ quadrupole mode, but also complex excitations to be described by *multiphonon* states.

In the neutron-proton (np) interacting boson model (IBM-2) [1], these multiphonon states are classified according to the quantum number F-spin [2–4]. The IBM-2 provides a specific signature for states of a given np symmetry. Strong $E2$ transitions connect the states with the same F-spin differing by one d boson, while states having the same number of bosons and different F-spin, called mixed symmetry (MS), are coupled by strong $M1$ transitions.

While the experimental evidence of the np symmetric excitations was well established for all nuclei long ago [5], only in the eighties the first MS state, the well known scissors mode [6], was observed in deformed nuclei [7]. Since then, the mode was identified in most deformed nuclei and thoroughly analyzed experimentally [8, 9] and theoretically [10]. Only recently, the existence of MS states in spherical nuclei was established experimentally. They were identified unambiguously for the first time in ^{94}Mo [11]. Few other experiments have established the existence of MS states also in the region around $N = 82$ [12, 13].

In most nuclei explored experimentally, the measured levels and transition probabilities fit well in the IBM-2 scheme. These low lying states have also been investigated theoretically within microscopic approaches. A shell model (SM) calculation has accounted for several properties of MS states [14, 15]. A more thorough investigation was performed within the quasiparticle-phonon model (QPM) [16–19].

The QPM, developed by Soloviev [20], consists in constructing a multiphonon basis out of phonons generated in quasiparticle-random-phase-approximation (QRPA). The basis so constructed covers a very large configuration space and, because of its phonon structure, is naturally related to semiclassical models and algebraic approaches as the IBM. In fact, the QPM multiphonon basis states can be viewed as the microscopic counterparts of the IBM bosonic states. Because of such a close link, the QPM can provide a microscopic support to the IBM scheme.

Apart from a QPM digression on ^{136}Ba, the region around $N = 82$ has been little explored. On the other hand, investigating those nuclei is of considerable interest not only for their intrinsic value, but also since recent experiments [12] have shown that the nuclear properties in this region do not change smoothly with the number of valence protons, suggesting important shell effects. Within QPM the properties of $N = 80$ izotones are discussed in [17, 21]

2 A Very Brief Outline of the Procedure

In the QPM procedure one assumes a Hamiltonian composed of a a Woods-Saxon one-body piece and a two-body potential which is the sum of several multipole-multipole terms. This Hamiltonian is expressed in terms of quasiparticle creation and annihilation operators, $\alpha^{\dagger}_{jm}(\alpha_{jm})$, obtained from the corresponding particle operators through a Bogoliubov transformation.

The quasiparticle separable Hamiltonian is then adopted to solve the QPRA eigenvalue equations to generate QRPA phonon operators of multipolarity $\lambda\mu$

$$Q^{\dagger}_{i\lambda\mu} = \frac{1}{2}\sum_{jj'}\left\{\psi^{i\lambda}_{jj'}[\alpha^{\dagger}_{j}\alpha^{\dagger}_{j'}]_{\lambda\mu} - (-1)^{\lambda-\mu}\varphi^{i\lambda}_{jj'}[\alpha_{j'}\alpha_{j}]_{\lambda-\mu}\right\} \tag{1}$$

and their energies $\omega_{i\lambda}$.

The quasiparticle separable Hamiltonian is then expressed into the phonon form

$$H_{QPM} = \sum_{i\mu}\omega_{i\lambda}Q^{\dagger}_{i\lambda\mu}Q_{i\lambda\mu} + H_{vq}, \tag{2}$$

where the first term is the unperturbed phonon Hamiltonian and H_{vq} is a phonon-coupling piece whose exact expression can be found in Ref. [20]. It is worth to point out that, among the QRPA phonons, only few are collective, composed of a coherent linear combination of two-quasiparticle configurations.

The phonon Hamiltonian is then accordingly diagonalized in a space spanned by states composed of one, two, and three QRPA phonons. The eigenfunctions have the structure

$$\Psi_{\nu}(JM) = \sum_{i} R_i(\nu J)Q^{\dagger}_{iJM}|0> + \sum_{i_1\lambda_1 i_2\lambda_2} P^{i_1\lambda_1}_{i_2\lambda_2}(\nu J)\left[Q^{\dagger}_{i_1\lambda_1}\otimes Q^{\dagger}_{i_2\lambda_2}\right]_{JM}|0> +$$
$$+ \sum_{i_1\lambda_1 i_2\lambda_2 i_3\lambda_3 I} T^{i_1\lambda_1 i_2\lambda_2 I}_{i_3\lambda_3}(\nu J)\left[\left[Q^{\dagger}_{i_1\lambda_1}\otimes Q^{\dagger}_{i_2\lambda_2}\right]_{I}\otimes Q^{\dagger}_{i_3\lambda_3}\right]_{JM}|0>, \tag{3}$$

where ν labels the specific QPM excited state of total spin JM. The wavefunctions are properly antisymmetrized according to the procedure outlined in [17, 20].

Each transition operator is composed of two pieces [22]. The first is linear in the $QRPA$ phonon operators $Q_{i\lambda\mu}$ and $Q^{\dagger}_{i\lambda\mu}$ and, therefore, connects states differing by one phonon. This is the leading term and promotes the *Boson allowed* transitions. The second piece links only states with the same number of phonons and promotes the *Boson forbidden* transitions. The first term is dominant in the $E2$ transitions. The second is responsible for the $M1$ transitions, which would be forbidden otherwise.

The used single particle basis encompasses all bound states from the bottom of the well up to the quasi-bound states embedded into the continuum. We adopted for the Woods-Saxon potential the parameters used previously for ^{136}Ba [17], which fit on average the single particle spectra of the $A = 141$ nuclei. The strength of the quadrupole-quadrupole interaction is fitted according to the procedure adopted in QPM [20, 22, 23].Because of the large model space, we used effective charges very close to the bare values. More specifically we put $e_p = 1.05$ for protons and $e_n = 0.05$ for neutrons. We also used the spin-gyromagnetic quenching factor $g_s = 0.8$.

3 Calculation and Results

3.1 QRPA Analysis

The first step is to ascertain that the low-lying QRPA spectrum contains, in addition to the np symmetric collective 2^+, with n and p amplitudes in phase, another 2^+ state which is fairly collective and is dominantly np non symmetric, with n and p amplitudes in opposition of phase.

In all studied nuclei ^{134}Xe, ^{136}Ba, and ^{138}Ce^{134}Xe, the lowest 2^+_1 is by far the most collective quadrupole state The second lowest 2^+_2 in ^{134}Xe and ^{136}Ba is fairly collective and has a np MS character, with the main proton and neutron amplitudes in opposition of phase. In ^{138}Ce, instead, there are two 2^+ states which get an appreciable $E2$ strength and have a dominant np MS character The third 2^+_3 is more collective and, therefore, is the best candidate for being considered the counterpart of the IBM-2 MS state.

This is a clear shell effect. Indeed, in ^{138}Ce the $1g7/2$ proton subshell is filled. Their low-lying excitations are therefore due to the diffuseness of the Fermi surface induced by pairing. The 2^+_3 in ^{138}Ce gets contribution from several proton configurations, made accessible by the diffuse Fermi surface. The corresponding state in the other two isotones is non collective. In the latter nuclei, since the $1g7/2$ proton subshell is only partially filled, the proton chemical potential is lower than in ^{138}Ce.

3.2 QPM Results

In all three nuclei, the first 2^+_1 is mostly accounted for by the lowest QRPA one-phonon component, although the amplitude of the two-phonon piece is appreciable,

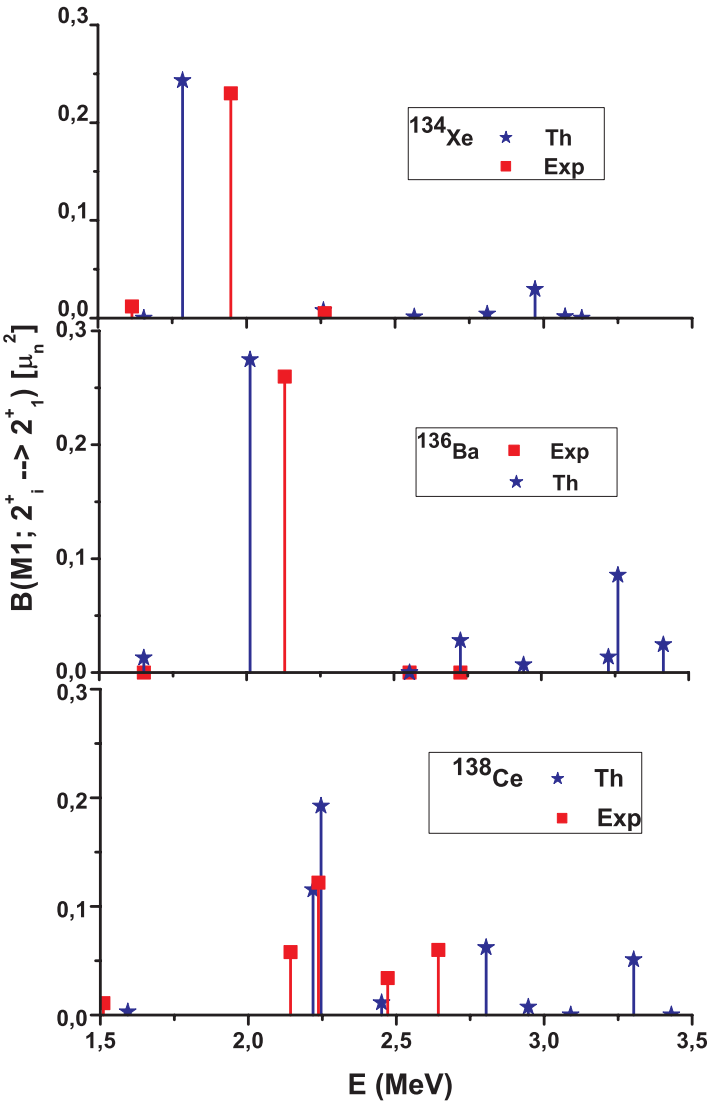

Figure 1. (Color online) QPM versus Experimental $M1$ strength distribution in ^{134}Xe, ^{136}Ba, and ^{138}Ce.

especially in ^{136}Ba. The second QPM state has a dominant two-phonon component in all three nuclei.

The other states mark a difference between the ^{138}Ce and the other two isotones ^{134}Xe ^{136}Ba. In the latter nuclei, the third 2_3^+ is dominated by the np MS QRPA phonon and corresponds to the MS state in IBM-2. In ^{138}Ce, the np MS QRPA phonon is shared by the 2_4^+ and, to a less extent, the 2_3^+. Both QPM states contain

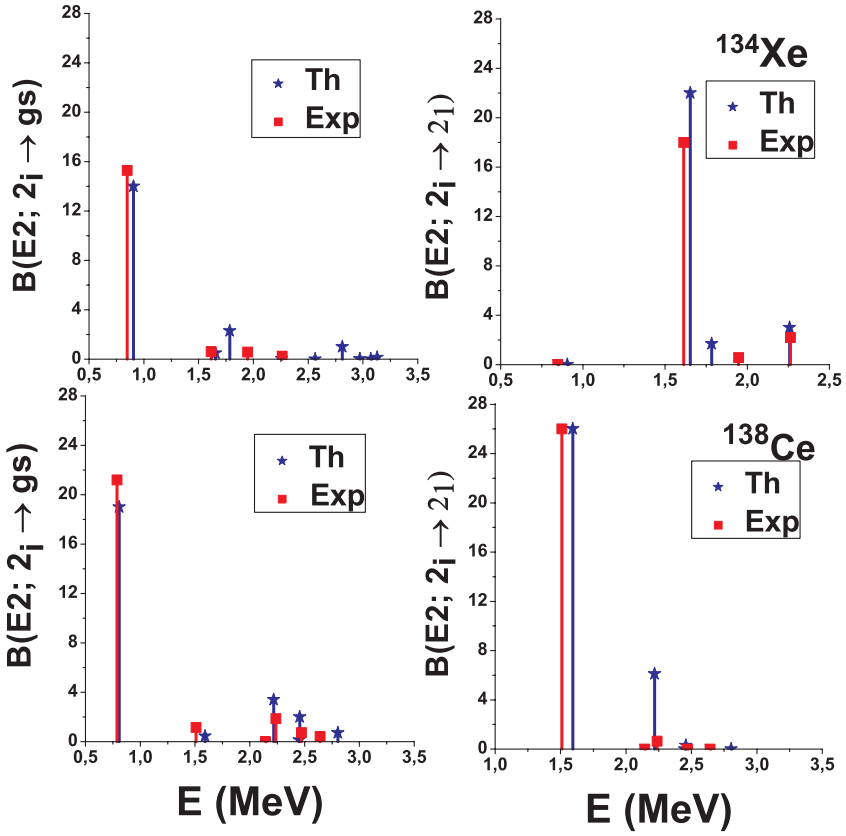

Figure 2. (Color online) QPM $E2$ strength distribution in ^{134}Xe and ^{138}Ce. ^{136}Ba has a similar behavior.

the second QRPA $[2^+_2]_{RPA}$ with an appreciable amplitude. We have pointed out already that in ^{138}Ce the quadrupole collectivity was shared by second and third QRPA 2^+ states, aside from the first one.

Apparently the interaction between these two fairly collective states lead to the generation of two QPM states with MS character. This is reflected in the $M1$ transitions . While in ^{134}Xe and ^{136}Ba we have one strong $M1$ peak (first and second panels of Figure 1), in ^{138}Ce the $M1$ strength splits into two peaks (third panel of Figure 1).

As Figure 1 shows, the main $M1$ peaks move upward in energy as the number of valence protons increases until the $1g7/2$ subshell is filled. The occupation probabilities of the higher energy shells increase thereby enhancing the diffuseness of the Fermi surface. This feature emphasizes once more the role of the shell structure in determining the properties of the low-lying states in open shell nuclei.

The agreement between the QPM calculation and experiments is good for both $M1$ and $E2$ strength (Figure 2) distributions. In particular the selection rules which

provide the signature for the np symmetry nature of the 2^+ states are fulfilled with high accuracy.

4 Concluding Remarks

The QPM investigation presented here has shown that the low-lying states observed in the $N = 80$ isotones can be well classified according to the np symmetry in agreement with the F-spin IBM-2 scheme. The splitting of the $M1$ strength observed in ^{138}Ce is shown to be due to the specific shell structure of this nucleus. Because of the proton $1g7/2$ subshell closure, the low-lying proton excitations are made possible by the diffuse Fermi surface induced by pairing. This leads to a higher number of low-lying states with MS character. Hence the splitting of the $M1$ strength.

This is a genuine shell effect which can be explained only within a microscopic context.

Acknowledgements

The present work was partly supported by the Italian Ministry of Instruction, University, and Research (MIUR) and by the Bulgarian Science Foundation (contract n. VUF06/05 and DAAD-09). Ch. S. thanks the INFN for financial support and hospitality. The authors thank N. Pietralla for useful information and discussions.

References

1. F. Iachello and A. Arima, *The interacting boson model*, (Cambridge University Press, Cambridge, 1987).
2. A. Arima, T. Otsuka, F. Iachello, and I. Talmi, *Phys. Lett.* **B 66**, 205 (1977).
3. T. Otsuka,A. Arima, and F. Iachello, *Nuc. Phys.* **A 309**, 1 (1978).
4. F. Iachello, *Phys. Rev. Lett.* **53**, 1427 (1984).
5. A. Bohr and B. Mottelson, *Nuclear Structure*, Vol. 2 (Benjamin, New York, 1975).
6. N. Lo Iudice and F. Palumbo, *Phys. Rev. Lett.* **41**, 1532 (1978).
7. D. Bohle, A. Richter, W. Steffen, A. E. L. Dieperink, N. Lo Iudice *et al.*, *Phys. Lett.* **B137**, 27 (1984).
8. A. Richter, *Prog. Part. Nucl. Phys.* **34**, 261 (1995).
9. U. Kneissl, H. H. Pitz, and A. Zilges, *Prog. Part. Nucl. Phys.* **37**, 349 (1996).
10. N. Lo Iudice, *Riv. Nuovo Cimento* **23**, 1 (2000).
11. N. Pietralla, C. Fransen *et al.*, *Phys. Rev. Lett.* **83**, 1303 (1999).
12. G. Rainovski, N. Pi etralla *et al.*, *Phys. Rev. Lett.* **96**, 122501 (2006).
13. T. Ahn, N. Pietralla *et al.*, *Phys. Rev.* **C 75**, 014313 (2007).
14. A. F. Lisetskiy, N. Pietralla, C. Fransen, R.V. Jolos, P. von Brentano, *Nucl. Phys.* **A 677**, 1000 (2000).
15. V. Werner *et al.*, *Phys. Lett.* **B 550**, 140 (2002).
16. N. Lo Iudice and Ch. Stoyanov, *Phys. Rev.* **C 62**, 047302 (2000).

17. N. Lo Iudice and Ch. Stoyanov, *Phys. Rev.* **C 65**, 064304 (2002).
18. N. Lo Iudice and Ch. Stoyanov, *Phys. Rev.* **C 69**, 044312 (2004).
19. N. Lo Iudice and Ch. Stoyanov, *Phys. Rev.* **C 73**, 037305 (2006).
20. V. G. Soloviev, *Theory of atomic nuclei : Quasiparticles and Phonons* (Inst. of Phys. Publ., Bristol and Philadelphia, 1992).
21. N. Lo Iudice, Ch. Stoyanov, and D. Tarpanov, *Phys. Rev. C* **77**, 044310 (2008).
22. V. Yu. Ponomarev, Ch. Stoyanov, N. Tsoneva, M. Grinberg, *Nucl. Phys.* **A 635**, 470 (1998).
23. M. Grinberg, Ch. Stoyanov, and N. Tsoneva, *Phys. Part. Nucl.* **29**, 606 (1998).